STAG: Smart Tools and Applications in Graphics (2023)
K. Lupinetti, F. Banterle, N. Capece, and U. Erra (Editors)

VarIS: Variable Illumination Sphere for Facial Capture, Model Scanning, and Spatially Varying Appearance Acquisition

J. Baron,[1] X. Li,[1] P. Joshi,[1] N. Itty,[2,1] S. Greene,[3,1] D. S. J. Dhillon,[1] and E. Patterson[1]

[1]Clemson University, Visual Computing Division, SC, USA
[2]Worcester Polytechnic Institute, MA, USA
[3]College of Charleston, SC, USA

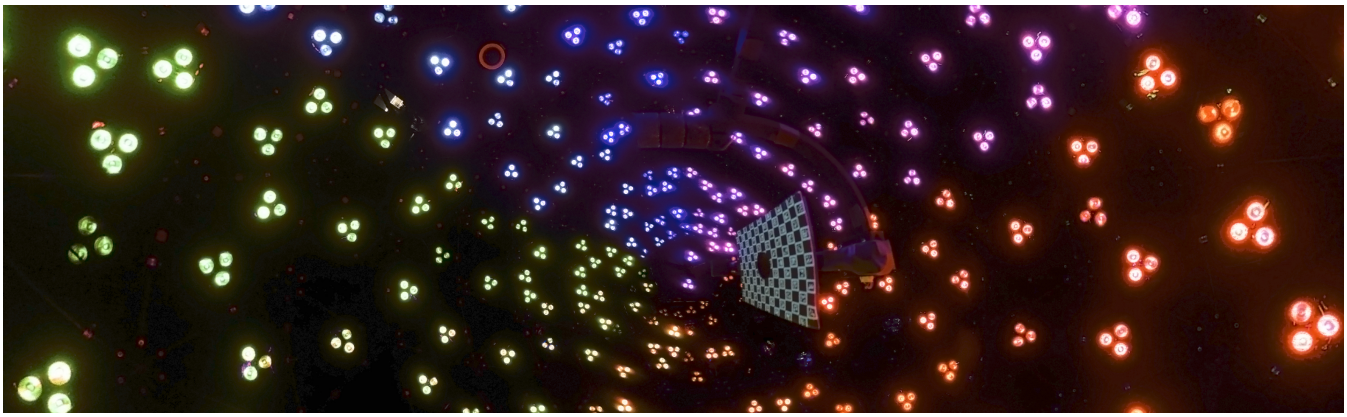

Figure 1: *Testing a 360-degree view from inside of VarIS with universal stage, sample plate, and ring-light apparatus (reflected) visible.*

Abstract

We introduce VarIS, our Variable Illumination Sphere – a multi-purpose system for acquiring and processing real-world geometric and appearance data for computer-graphics research and production. Its key applications among many are (1) human-face capture, (2) model scanning, and (3) spatially varying material acquisition. Facial capture requires high-resolution cameras at multiple viewpoints, photometric capabilities, and a swift process due to human movement. Acquiring a digital version of a physical model is somewhat similar but with different constraints for image processing and more allowable time. Each requires detailed estimations of geometry and physically based shading properties. Measuring spatially varying light-scattering properties requires spanning four dimensions of illumination and viewpoint with angular, spatial, and spectral accuracy, and this process can also be assisted using multiple, simultaneous viewpoints or rapid switching of lights with no movement necessary. VarIS is a system of hardware and software for spherical illumination and imaging that has been custom designed and developed by our team. It has been inspired by Light Stages and goniophotometers, but costs less through use of primarily off-the-shelf components, and additionally extends capabilities beyond these devices. In this paper we describe the unique system and contributions, including practical details that could assist other researchers and practitioners.

CCS Concepts

• ***Computing methodologies*** → ***Reflectance modeling; 3D imaging;*** • ***Hardware*** → *Emerging optical and photonic technologies;* • ***Applied computing*** → *Media arts;*

Keywords: Facial Capture, Photogrammetry, Material Acquisition, Appearance Capture

1. Introduction

As computer graphics has improved significantly over the decades, the drive for better representing our physical reality has been a main

theme of work. With improvements, the desire to use real-world data directly in graphics applications or in building better models to serve both graphics and other areas of research only increases. Efficiently acquiring that data is still an ongoing area of work and one that has been facilitated by recent developments in commercial production of light-emitting diodes (LEDs), higher quality but less expensive imaging devices, accessible micro-controller platforms, computer-aided design (CAD) software, 3D printing, etc. Inspired by a variety of other capture devices from the Light Stages [Deb12a] to goniophotometers and others [GG18], we have developed a unique and relatively low-cost device using commodity components that is able to function similarly to those but with novel capabilities. It additionally can serve as a practical system for production-centric acquisition. In this paper we present a brief survey of material that has helped inform our thinking followed by design choices and implementation details that may be of benefit to others.

2. Background and Related Work

2.1. Faces

Photo-realistic rendering of the human face requires acquisition of detailed geometry and associated texture maps for encoding spatially varying structural and reflectance details, preferably in a musculature-inspired, well-formed, and consistent topological layout. Facial representation such as this is tremendously useful in visual-effects and game production as well as research in a variety of fields; however, the development of a high-quality model remains a laborious task, encompassing face detection, key-point landmarking, geometry acquisition, alignment and correspondence, reflectance acquisition, and re-topologizing – all steps often guided or completed with human artistry. The predominant approach for face-geometry acquisition is multi-view stereo (MVS) reconstruction which entails the capture of multiple images of a subject from various vantage points, processed through camera calibration, image rectification, feature matching, solving for depth maps and 3D point clouds, and mesh construction. Several instrumental devices, such as the Cyberware facial scanner, have been used historically. That particular device solved the multi-view correspondence problem actively by using low-intensity lasers to corroborate surface points in different views with high fidelity [ZZG07]. Similarly, the commercial 3DMD face scanners adopted an active multi-view stereo methodology, with projection of infrared light patterns to aid solving correspondence [3dm22]. In contrast, passive multi-view stereo setups avoid additional active illumination beyond that needed to expose facial images. Beeler et al. proposed such a facial-reconstruction pipeline and leveraged skin-specific assumptions with multi-view images and a “dark is deep” technique to obtain high-quality captures with plausible meso-structure [BBB*10]. Much of very recent work related to face capture attempts to infer such detail from single frontal images, often using machine-learning, but we limit discussion here to methods rooted in accurate, detailed physical measurement. Likely the most influential face-capture related work has been that by Paul Debevec and team at the University of Southern California Institute of Creative Technologies (ICT) [DHT*00; Deb12a]. While MVS techniques are used during their various implementations of face capture, the primary contributions have involved photometric techniques for acquiring high-quality reflectance and sub-millimeter detail of the face. Some of their influential work includes the use of gradients based on the first four spherical harmonics to estimate surface normal maps at high detail and cross-polarization states for calculating diffuse and specular albedo maps [MHP*07; GFT*11]. Additional multi-spectral techniques have been employed to improve accuracy and efficiency [LBK*18]. As an alternative to cross-polarization, Kampouris et al. at Imperial College London (ICL) introduced a method for view-independent diffuse-specular separation of albedo and photometric normals using binary spherical gradient illumination [KZG18].

The nature of complex, unordered meshes from multi-view stereo techniques necessitates subsequent steps of model correspondence as well as re-topology for rigging and animation purposes. The influential 3D face modeling technique of 3D morphable models (3DMM) by Blanz and Vetter and work inspired by it has often solved alignment and correspondence with automated landmarking, texture-mapping, and a non-rigid iterative closest point algorithm, but musculature-inspired topology has not been a concern for much of the work [BV99; ARV07]. Other work has provided semi-automated methods for devising correspondence with well-formed geometry to create good topology under a common ordering [IAD13; PBS18; LLB*21]. In production, this is still typically solved semi-manually using commercial software tools.

Methods for acquisition of geometry and reflectance data, high-quality correspondence and re-topology, and population face models continue to be an active area of research. Various devices have facilitated work in this area; VarIS draws particular inspiration from the Light Stages [Deb12b]. Initially designed to capture the reflectance field of the human face, the Light Stage concept has evolved over time and inspired other devices. Weyrich et al. constructed a similar apparatus featuring 16 digital cameras and 150 LED light sources for work in face and skin-reflectance capture [WMP*06]. Ghosh et al. at ICL introduced a versatile multi-spectral LED sphere comprising 168 RGB and color temperature-controllable white lamps, as documented in [KG18]. Zhang et al. at ShanghaiTech University constructed FaStage, geared at high-speed face capture for dynamic processing [ZZZ*22; ZZC*23].

2.2. Model Scanning

Several image-based methods for scanning 3D geometries using multiple views have been developed including disparity from MVS, texture features, motion, shading under controlled illumination, silhouettes, focal changes, structured light, and photogrammetry. Refer to the review by Remondino & El-Hakim [RE06] for more details and categorization based on active or passive sensor approaches. Recently, computational-photographic methods using coded-apertures, micro-lens arrays as well as meta-surfaces are devised for highly specialized applications in 3D scanning, including those at microscopic levels. While some strategies are beyond the context for our developed setup, we discuss those strategies that are closely related to our work. VarIS is designed to house such modalities to provide model-scanning capabilities.

Photogrammetry and Multi-view Geometric Reconstruction: Widely used for cultural heritage preservation and archaeology, photogrammetry involves taking multiple photographs of an object from different angles and using algorithms to reconstruct 3D structure. It relies on image-based feature-detection algorithms to match a sparse set of correspondences across views. Using projective geometry we then back trace a pair of rays for each pair of pixels that correspond across two views for one individual feature point. For this step, we first pre-calibrate the camera pairs for determining their intrinsic parameters and relative extrinsic placements. Tracing the rays backwards to intersect them (triangulation) gives the 3D point location of the given feature point. Multi-view reconstruction techniques involve capturing an object from various viewpoints and using computer vision algorithms to reconstruct its 3D shape [SD99; PSQ06]. Hartley & Zisserman [HZ03] provide an in-depth exposition. However, under fixed illumination, extracting finer geometric details is often complicated; photometry or structured-light techniques provide means to actively control illumination to further extract detail.

Photometry: Photometric stereo techniques capture surface normals by observing a given object under varying lighting conditions, and these normals can then be integrated to form a detailed 3D model [Woo80]. As a prerequisite, photometric methods often require a single camera and multiple known locations for point-light illumination of fixed intensity. Assuming that the surface is uniformly diffuse and there is only one light direction at time, we can relate each pixel's observed intensity to its surface normal. With such constraints one can solve for the corresponding surface normal without the need for knowing the illumination intensity or camera parameters. Next, imposing these surface normals as constraints on relative locations of surface points corresponding to adjacent pixels, we solve for the 3D mesh. For further detail refer to [Woo84]. Ackermann & Goesele [AG*15] provide a good survey of general approaches for photometric reconstruction. Also, Shi et al. [SWM*16] provide a benchmark dataset, classification, and quantitative evaluation of several existing photometric methods with greater focus on examining non-diffuse surfaces under unknown illumination.

Structured Light Scanning: Structured light scanning techniques are commonly used for capturing the geometry of physical objects that may vary greatly in their reflectance characteristics. These methods project a known pattern onto the object's surface and analyze its deformation to calculate the 3D shape. In principle, they aim at imposing an unambiguous grid of an "illumination" texture to codify the view frustum by projecting a unique pattern through each pixel on a projector device which dominates the scene illumination. Such patterns can be temporal or spatial and can be decoded in each camera's view-space to establish unambiguous correspondence across multiple views.Structured-light scanning systems require calibrating a pair or more of cameras. Furthermore, one of the cameras can be replaced by the projector since its optics also follow the pin-hole model, albeit in reverse [MT12; DG15]. Structured-light systems can scan 3D geometries robustly [MT12; ZXX*14], with high accuracy (sub-millimeter scale) [DG15], with high flexibility and speed [HTOL20], as well as at low costs [RCM*01]. They are popular across a wide range of applications, including production quality inspections [PG07], robotics [LBSG22], cultural-heritage digitization [ARN*06], as well as gaming and consumer products such as Microsoft's Kinect Camera [Zha12].

2.3. Materials

Here we present a brief overview of materials for graphics and how systems such as VarIS may be designed for their acquisition. Surveys by Weyrich et al. [WLL*08] and Guarnera & Guarnera [GG18] summarize in more detail the variety of material-function representations and data-capture methods.

2.3.1. BxDFs

The Bidirectional Reflectance Distribution Function (BRDF) is a mathematical model introduced in optics for describing the ratio of extant radiance to incident irradiance. Guarnera & Guarnera state [GG18] that the most general function has 16 variables: (1, 2) incident and extant wavelengths, (3, 4) incident direction (as spherical coordinates) of light arriving at surface, (5, 6) extant direction of light, (7, 8) transmittance direction through the surface, (9, 10) times ray hits and exits surface, (11, 12, 13) a 3D spatial location on surface at intersection point, and (14, 15, 16) a different extant surface 3D location. The first 8 (the wavelengths and directions) typically have the most impact in modeling surface appearance and are the most practical to include in a capture system.

Early work [TS67; CT82] introduced the microfacet BRDF which assumes that a surface is composed of many mirror-like facets arranged according to a Normal Distribution Function (NDF), driving whether a surface appears rough (diffuse) with highly random microfacet orientations or smooth (specular) with more aligned microfacets. To generalize for BRDF variations, "BxDF" is often used, where the x can stand for additional terms. For example a Bidirectional Transmittance Distribution Function (BTDF) includes the transmittance direction parameters, and the BSDF combines the BRDF and BTDF to describe light scattering in any direction. Many simulations simplify wavelength to red, green, and blue values. More spectral sampling could provide a better means of emulating effects such as structural-coloration or fluorescence. Accounting for spatial dimensions to describe surface locations is key to describing phenomena such as subsurface scattering (BSSDFs) where light enters, bounces within, and exits from a surface at a likely different location with a different spectral intensity and value.

The Spatially Varying BxDF (SVBxDF) adds the 3 additional parameters for designating a spatial location on the surface to account for features that vary across the surface and contribute to its appearance. (If the surface is assumed to be flat, then only 2 dimensions are sufficient.) The spatially varying BRDF (SVBRDF) or BSDF (SVBSDF) can best represent natural phenomena which always exhibit such features that are difficult to simplify with uniform analytical models. Therefore, our appearance-capture pipeline for VarIS is focused on SVBSDF capture. A Bidirectional Texture Function (BTF) also models spatial information but is a data-heavy representation describing an Apparent BRDF (ABRDF), which includes self-shadowing and self-occlusions, explicitly per directional combination per spatial location. Further BxDF variations

exist such as changing the underlying geometry (i.e. curved surfaces as BCSDFs) and layered material models, but for this work we focus on the 16-dimensional model representation by Guarnera & Guarnera with an emphasis on the directional, wavelength, and simplified spatial parameters.

2.3.2. Material/Appearance Capture

Measuring the appearance of a surface entails gathering detailed measurements of scattered radiant energy and relies on the BxDF parameterization and practical limitations of the system. Key components of a capture system include light sources, sensors, and the angular resolution or rotational capabilities of the structure.

Illumination: Illumination for a capture system involves geometric and radiometric properties. The location, direction, and shape of the light affect the incident directional irradiance resolving a given parameterized BxDF. Common approximations include lights being modeled as "point lights" to resolve specular interactions and diffuse lighting being modeled as "ambient lighting" to estimate diffuse scattering. Klehm et al. [KRP*15] provide an excellent review of various geometric configurations used for efficient appearance captures. Other important aspects include spectral profile, net power, and polarization. Broad-band daylight (such as a D50, D55, or D65 profile) is desirable but difficult or expensive to build in hardware. As an alternative, several narrow-band LED units along with few broader-band white-like lights are commonly employed for capture setups like light stages: one narrow channel for each of red, blue, and green bands and three white-like profiles (cold, natural, and warm) [LYL*16; KG18]. Larger setups require additional power to allow for high-speed and low-noise acquisition. Commonly, two sets of light sources are polarized linearly in opposite configurations to ease separation of diffuse and specular appearance parts through polarized filtering in front of the camera [KG18] though this increases the net lumen requirements.

Figure 2: *VarIS with all white lights activated.*

Sensors: The most common photometric sensors for material-capture systems are spectrometers and digital camera (CCD) sensors. Spectrometers are sensitive to a single wavelength at a time and measure highly precise radiometric values at that given wavelength at a certain surface point. Camera sensors are typically designed for detecting and measuring red, green, and blue radiant energy often on a Bayer grid favoring green like the human visual system. The grid-based sensors provide spatial information which is needed to be able to measure SVBSDF data.

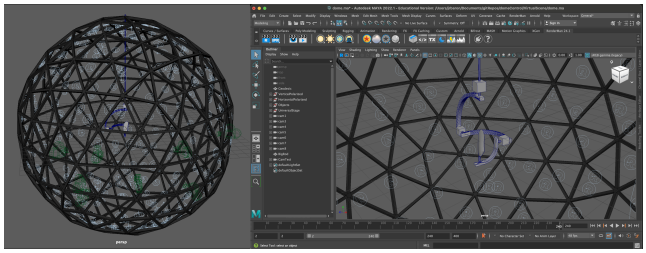

Figure 3: *Simulated VarIS, used to aid research and development.*

Structures, Gantries, and Turntables: One major consideration of a system is how lights, sensors, and sample are arranged for greatest angular resolution. The arrangement can be fixed on a rigid hemispherical or spherical structure, or the accessories can be affixed to rotational gantry arms. The rigid structure may be geodesic (a nearly complete sphere like the later ICT Light Stages [Deb12a], hemisphere geodesic structures like in [MGW01], a complete geodesic sphere like VarIS shown in Figure 2), or composed of latitudinal and longitudinal arcs (as with ICL's light stage [KG18]). Other systems may not have an external structure but rely on movable gantry arms for controlling angular resolution. Combining both a rigid hemispherical or spherical structure and movable components can further maximize the angular resolution with the rotations of gantries or turntables filling in gaps from the accessories mounted on the rigid structure.

Material Parameterization and Representation: The BxDF parameterization drives the appearance-capture setup and data representation particularly in choosing the directional parameters. For a simplified BRDF, consider only the incident direction based on the light source and the extant direction based on the sensor and both in respect to the orientation of the material sample. The light sources, sensors, and sample orientation should be configured in a way that allows for arranging each accessory in any possible combination of directions. For a BSDF, the direction of transmittance also has to be considered in terms of the system's capability to align the light source and sensor on opposite sides of the material sample. Each system has a scheme for taking measurements in a controlled manner at many different combinations of lighting and viewing directions which are, ideally, selected in order to measure the most important scattering features of the surface such as specular, mirror-like highlights which may be missed or misrepresented with insufficient sampling frequency. Rusinkiewicz proposed the half-difference angle parameterization of the isotropic BRDF [Rus98] to reduce the four dimensions down to three; the system used for the MERL material study [MPBM03] is based on this parameterization. A recent BRDF-capture system proposed by Dupuy & Jakob is based on an adaptive parameterization leveraged during both capture and rendering but does not capture spatially varying properties [DJ18]. Designing a system for SVBRDF and

BTF capture requires accounting for at least two spatial dimensions identifying a point on the sample surface. Camera sensors are better equipped for geometric calibration and defining spatial dimensions. Subsurface scattering further accounts for separate locations for light entering and exiting a surface. Systems include Weyrich's for studying skin subsurface scattering [WMP*06] and the DISCO system for acquiring translucent materials [GLL*04].

Based on these main categories of components, different trends in system designs have emerged. In general we present the following categories of systems: goniophotometers, large-scale image-based systems, and small-scale image-based systems or handheld devices. Goniophotometers are designed typically with a single light source, a spectrometer as a sensor, and holder for the material sample with at least one of these components able to rotate. The key goniophotometer-based study that influences our work is Dupuy & Jakob's [DJ18] which uses a pab-PG2 goniophotometer [Api10] that has a fixed light source, a spectrometer mounted on a 2-axis gantry arm, and a large sample plate with 2 degrees of freedom for setting orientation.Image-based systems may be based on gantries or spherical structures. Harvey et al. [HBM13] measured SVBSDF data with the Cornell Spherical Gantry which is based on the design of the Stanford Spherical Gantry used for Rusinkiewicz's BRDF study [Rus98], Jensen's skin study [JMLH01], and Marschner's hair study [MJC*03]. Light Stage systems [Deb12a; KG18] are equipped with a variety of light sources and cameras to capture the reflectance properties of materials under controlled lighting conditions. Smaller image-based systems have been used for gathering BRDF, BSSDF, SVBRDF, and BTF data. Such systems can offer more rapid, simultaneous data acquisition based on the spatial dimensions inherently captured by the camera sensors and with geometric tricks such as modifying the sample geometry. For example Marschner's image-based BRDF-acquisition setup [MWL*99] can leverage flat planar geometry and spherical samples. Inspired by this work, the minimal system created for the MERL study [MPBM03] assumed spherical samples of a wide variety of isotropic materials to sample from as representing many different directions and installed a stationary camera and a light source attached to an arm on a turntable.

3. Design and Implementation

3.1. Constraints

In an ideal system, one could generate a continuous, full-spectrum of wavelengths and measure those accurately from any viewpoints simultaneously over a large-volume light field with no undesired inter-object scattering interactions. Practically, though, we have to accept a certain number of design constraints, particularly including cost. Primarily using commodity components, many of which were not available several years earlier, combined with open-source software libraries and select custom-designed and fabricated components allowed us to reduce costs and development time. We needed the device to capture human-scale objects but still fit within university space constraints, and we needed a structure that minimized cost so that more funds could be spent on illumination and imaging. The structure still needed to support several-hundred pounds in lights and cameras without degradation or significant movement. Illumination needed to be sufficient, even under significant reduction due to polarization filtering, to capture moving humans in sharp images with fairly deep focus and low-noise but still be powered by few breakers on a typical building power system. High-resolution cameras and lenses that could capture pore-level detail on faces as well as track small-scale spatially varying points on surface materials were desired but at as low cost as possible. Exposure latitude for best capturing specular highlights that are orders of magnitude larger than typical reflectance with as few exposures as possible was important, as was maintaining an accurate color workflow. Cost limited the initial system to RGB Bayer-sensor cameras that are primarily visible-light spectrum sensitive.

Figure 4: *4V geodesic kit from Sonostar assembled with systematic installation of lighting beginning.*

Figure 5: *Lights, communication cabling, and power wiring during construction.*

3.2. Hardware

3.2.1. Structure

Before construction, we simulated the setup in Autodesk's 3D software Maya [Aut] and the RenderMan path-traced renderer [CFS*18] to facilitate testing and development, shown in Figure 3. The physical support structure is 4V geodesic of 8-foot diameter, designed and cut by Sonostar Universal Structures [Son]. The higher-frequency geodesic enabled a stronger, more spherical mounting grid for lights and cameras but at less cost than custom metal construction. The geodesic was raised slightly above the floor to facilitate keeping the bottom of the sphere and lights there that similar devices usually lack; a hinged door was created on one side of the structure for entry. The structure before most devices were mounted may be seen in Figures 4 and 5. Custom structures have been designed for the sample stage, ring-light mount, laser mount,

and turntable in CAD software. Each was tested with in-house 3D printing, and stage parts were ultimately fabricated in aluminum by Craftcloud [Pli].

3.2.2. Illumination

A myriad of options were evaluated relative to cost, exposure, spectrum, speed, power, and mounting constraints, and off-the-shelf DMX-based lights were ultimately chosen. There are 364 lighting units that each have red, green, blue, and white LEDs on each single package (RGBW) collimated by a Fresnel lens, three to a unit. We opted for as many as possible within cost and mounting space and a layout of latitudinal and longitudinal arcs, mounted as closely as possible over the geodesic, to aid setup of two sets of polarization that could be switched easily as in earlier work [MHP*07]. Physical mounting near the poles was challenging, and we added additional structural rings to assist. The combined LEDs offer a good coverage of the visible range of wavelengths and capabilities for spectral variation; spectral power distributions are shown in Figure 6. LED lighting operates cooler and at lower power than traditional lighting options, but power is still a concern with so many devices. The light units require roughly 15W each at maximum output. To work within the 15-20 amp range of building electrical breakers, each power group was kept to about 11 amps (91 light units) for a safety factor while also limiting to four power groups, each distributed to outlets supplied by different breakers.

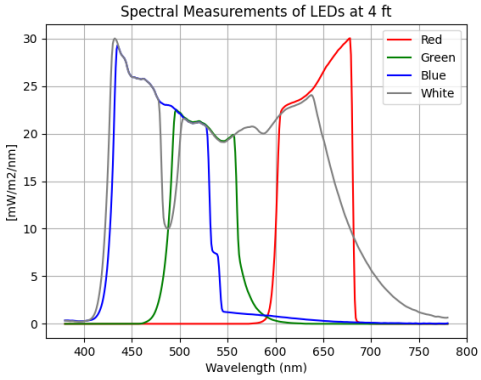

Figure 6: *Spectral power distribution (SPD) of the red, green, blue, and white LEDs measured from the center of VarIS.*

Additionally, accessories have been constructed particularly for retroreflection, where the light and view orientations are aligned. These include a 532nm laser (Figure 7) and a white ring light attached to a camera lens (shown for display purposes in Figure 10). We designed and 3D-printed a custom mount to align the laser and a 50-50 beam splitter in front of the lens. Half of the laser's radiant energy directs to the center of VarIS and half onto a beam dump, also enabling the radiance reflected from a mounted material to return through the beam splitter and camera optics.

3.2.3. Imaging

VarIS's imaging employs camera "raw" formats and is manufacturer agnostic in camera control, using the open gPhoto2 library [WNRM15] versus proprietary SDKs that limit device options and can be more subject to change. Currently VarIS workflows use Nikon (NEF) photographs but have also been tested with the Canon (CR2) format. We have additionally tested a 360-degree Ricoh Theta camera for calibrating LED positions and providing images such as Figure 1. There are now 16 Nikon D3500 cameras, chosen as a low-cost option that still has a high resolution (24MP), low-noise sensor without an optical low-pass filter (employed on many cameras to reduce aliasing but at the loss of detail). These also have video capabilities. We have chosen 85mm f/1.8G Nikkor lenses for face capture, as they frame a head-sized region and maintain low distortion and high-resolution, being one of the sharpest lenses manufactured by Nikon, and Nikkor 75-300mm f/4.5-6.3G ED lenses for close-focus distance that allows for a high-reproduction ratio, framing just the sample plate area (interestingly this was one of the least expensive but best options for telephoto lenses in the 300mm range). Polarization filters may be attached to reach cross-polarized states through switching light sets.

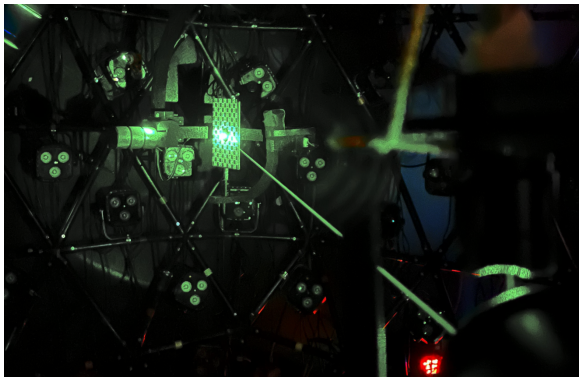

Figure 7: *The beam from a 532nm laser aligned with the camera and a material sample for measuring retroreflection.*

3.2.4. Communication

Closely related to lighting, we also considered options for communication. The ESTA DMX512A lighting standard was chosen as a well supported, off-the-shelf system that could meet reliability, control a large number of devices, and also reduce cost by requiring fewer custom electronics [ANS]. The choice came with the loss of very high speed operation, though, as the standard has a relatively slow maximum switching speed of 44Hz. We confirmed this during empirical testing, as light-activation aliasing occurs with packet loss above that rate. The rate is still sufficient to complete most work of interest but unfortunately limits high frame-rate video-capture techniques. DMX documentation [Ben08] also suggests limiting the number of devices on each serial chain for reliability. We thus wired, numbered, and programmed 6 serial chains with 36 light units on each chain and 4 additional serial chains that included a top or bottom pole of the two different polarization states, for the total of 364 light units. Arduino DMX boards and control boxes were tested, but the most cost effective and reliable solution at the time was the USB-DMX Adapter cable by DMXKing with serial conversion built into the connector. Distributed systems were considered, but a central computer was preferred for all control and

processing. Two 20-port USB hubs were employed to drive serial communications for both the lighting as well as the camera, motorized systems, and accessory illumination control. Quality cabling is needed, particularly for long runs for camera control. We have still had occasional camera communication disconnects that we believe may be caused by the USB hubs and are considering testing PCI-based USB expansion cards. A custom serial packet system was devised for motorized systems and accessory lighting control and interpreted via Arduino boards to drive stepper-motor controllers or relays for accessory lighting power.

Figure 8: *Sculpture on automated turntable, polarized illumination (viewing camera not cross-polarized here).*

3.2.5. Automated Turntable

The automated turntable (photographed in Figure 8) uses a traditional sculpture turntable for an off-the-shelf build with quality bearings. 3D printed parts were designed for support and to drive the turntable via NEMA-23 stepper motor. With the micro-step capability of the controller and motor combination, a large number of very small, incremental rotations can be smoothly and reliably executed even with fairly heavy items. The turntable can be installed or removed easily.

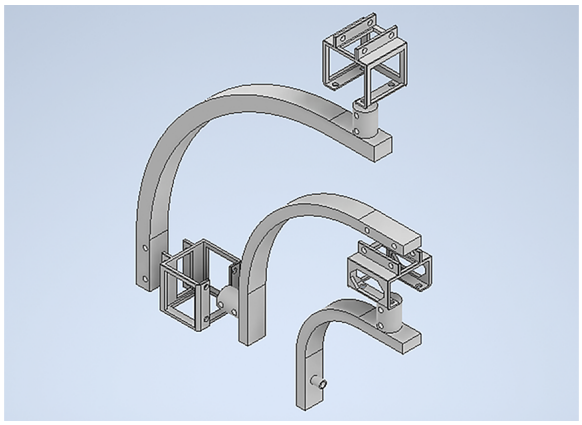

Figure 9: *CAD design of the universal-stage components.*

3.2.6. Motorized Universal Stage

We designed a motorized universal stage to orient material samples in VarIS's center to achieve fine angular resolution not typical for material capture in Light Stages or related devices.The stage is hung by a steel rod, tensioned to dampen vibrations, that can be easily removed to switch the "capture mode" of VarIS to the facial-capture or model-scanning applications. Figure 9 shows a render of its core components in CAD software. The 3-axis design enables Euler rotations about local X (right), Y (up), and Z (forward) axes, each physically consisting of a NEMA 17 stepper motor and a curved arm connecting to the child axes or sample mounts. We desire as few obstructions as possible such as an arm blocking light during transmissive capture, and alternative orientations can be achieved by the 3-axis design for capturing scattering data in any possible combination of directions. Motor holders are designed to dissipate heat. Components were designed in CAD software and ultimately 3D-printed with aluminum which is both lightweight, heat-resistant, and durable. Earlier tests made with plastic filaments (such as PLA and polycarbonate) had imperfections and flexed under heat. Counterweights on each arm reduce the the motor torque required, allowing smoother movement and reduced operating temperature, also facilitating material-capture sessions that may last more than a day. The sample holder is interchangeable for securing different material samples and is marked for calibration, inspired by the work of Harvey et al. [HBM13]. The sample holder currently uses a magnetic attachment and has a matte-surface tracking-marker board. The finalized structure (in Figure 10) is painted matte black with BLACK 2.0 paint.

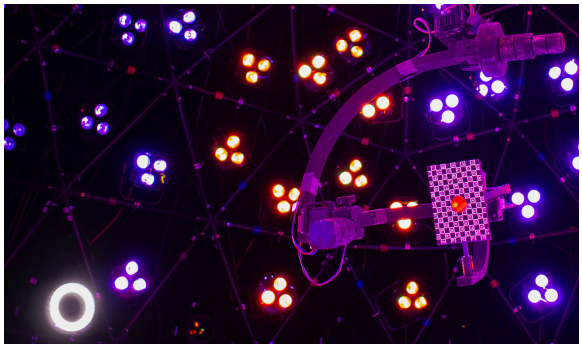

Figure 10: *Clemson-themed light display, demonstrating ring light, motorized universal stage, and calibration sample holder.*

3.3. Software

VarIS software, from core device communications to algorithms for specific capture sequences, is authored primarily in Python for speed of development, multi-platform deployment, and access to a wide variety of open-source libraries. Primary use libraries include built-in utility modules for file-system operations; pySerial [Lie] and gPhoto2 [WNRM15] for device communication; Qt5 [Coma] and PyQt5 [Comb], OpenGL [Gro], and mayapy [Aut] for user interfaces and visualizations; and NumPy [HMvdW*20], SciPy [VGO*20], OpenCV [Bra00], Colour [MMP*22], and Pandas [pdtea20] for data processing.

The "Lights" sub-module consists of pySerial opening serial ports to the 10 DMX chains for communication with the LEDs. This subsystem also sets a variety of illumination patterns such as axis gradients and one-light-at-a-time (OLAT) along with managing spatial coordinates per light. Communication with the laser and

ring-light devices is available via Python through custom wiring and a relay, an Arduino UNO board and script, and pySerial. The "Cameras" subsystem primarily uses gPhoto2 for camera control involving property-setting commands for establishing exposure settings and the image data format. Using Python's threading packages, we achieve synchronized, multi-camera captures with parallel communication. The universal stage's subsystem handles control with the NEMA stepper motors through pySerial and Arduino as well as converting angular values ultimately to instructions on the Arduino for executing safe rotations and managing orientations per stage arm and sample holder. We additionally have a module dubbed "Action" (*"Lights, Cameras, ...Action!"*) that contains the highest level of control code for unifying the sub-modules.

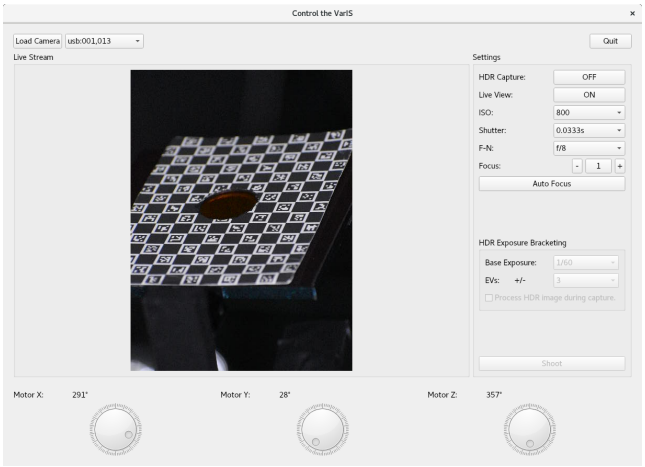

Figure 11: *Live-view camera control with Python, Qt, and gPhoto2 facilitates setup such as face and material-sample alignment.*

3.3.1. Acquisition

We developed a graphical user interface (GUI) (shown in Figure 11) based on PyQt5, gPhoto2, and OpenCV to display live camera views from the active devices to assist setup such as fine focus adjustment, testing exposure ranges, directing a person's face location in camera views, and aligning the material sample holder with a particular viewpoint. Software drives acquisition sessions that are discussed later per workflow. Captured images can be transferred from the camera SD cards to a destination file system either in one batch at the end of a session or periodically in smaller batches during the session. Exposure presets have been determined and may be selected manually or eventually automated given the capture technique being employed with the goals of keeping sharp focus across as much depth-of-field as possible, and keeping noise low by minimizing sensor gain (ISO) and using optimal aperture sizes of a lens. Bracketing can be set for capturing high-dynamic-range (HDR) data. Focus bracketing is also available in order to focus-stack imaging for improved photogrammetry.

3.3.2. Processing

Post-processing may include HDR merging, focus stacking, and image rectification. We leverage the Colour package [MMP*22] for HDR processing to produce OpenEXR 32-bit floating-point images. A custom color-correction technique can be applied for further obtaining images suitable to use as radiometric data [DJBP23]. Image rectification transforms image pixels from a source image to another view point based on calibrated camera matrices and is useful for processing orientations for material capture as well as tracking pixels for measuring spatially varying surfaces. We use OpenCV [Bra00] for detecting markers of a ChArUco board on the sample holder, estimating camera parameters, computing homography matrices, and transforming images.

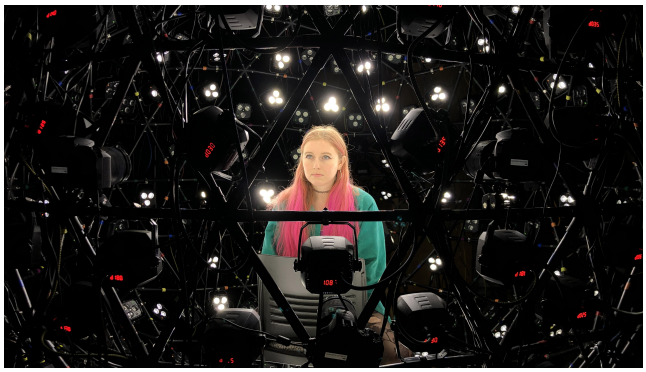

Figure 12: *View outside of VarIS during test face-capture session.*

3.4. Facial-Capture Workflow

We have implemented gradient-illumination and polarization strategies [MHP*07; GFT*11] for efficient texture acquisition and plan to implement more recent spectral and binary methods [LBK*18; KG18] with interest in continuing to refine capture efficiency and capabilities as well as develop new methods. We take 5 photographs in quick succession: under X-, Y-, and Z-gradient patterned illumination and under uniform and cross polarization. Figure 12 depicts an outside view of a face-capture test, Figure 13 shows example photographs under varying illumination patterns, and Figure 14 displays processed textures and renders.

Figure 13: *A sample of photographs taken under different photometric conditions within VarIS.*

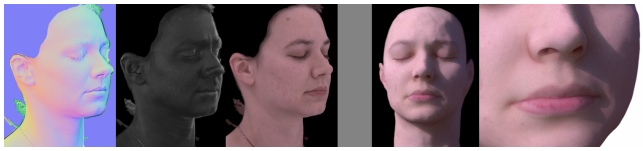

Figure 14: *Normal, specular, and diffuse albedo maps from one capture viewpoint (left images) and path-traced renders after photogrammetry (right images).*

We automatically mask images per viewpoint to remove non-facial information such as the background. We use Agisoft

Metashape [Agi] for photogrammetry as well as transforming specular, diffuse, and normal information extracted from photos into texture maps. We have been developing our own version of a face-specific capture method inspired by Beeler et al. [BBB*10], and we hope to compare and refine with the goal of improving capture methods and directly generating a high-quality common-topology mesh and associated maps for each capture. An example of path-traced renders of early capture results are shown on the right side of Figure 14. We retopologize the initial mesh to a standard, animatable mesh using Wrap [Fac] involving texture-map transfer. From there the mesh and associated textures can be transferred to production environments including the real-time Epic MetaHuman plugin [Gam]. Both transfers are shown in Figure 15.

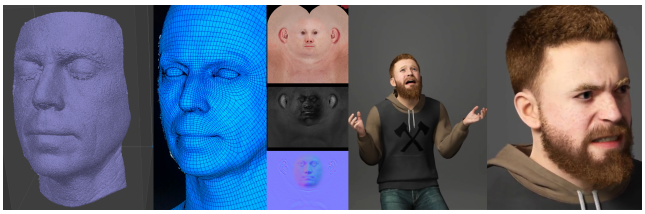

Figure 15: *Left half: From early VarIS capture to standardized, animatable mesh using Wrap by FaceForm [Fac]. Right half: From VarIS capture to Epic MetaHuman [Gam].*

3.5. Model-Scanning Workflow

Scanning a model in VarIS involves taking hundreds or thousands of photographs at small rotational increments with the option of setting patterns of illumination as those used for the facial-capture workflow for additional textured appearance information. Cross-polarization improves results by removing most view-dependent specular effects that interfere with finding correspondence among photographed object points. Figure 8 shows a model, a sculpture of a witch's head, resting on the turntable for automated scanning.

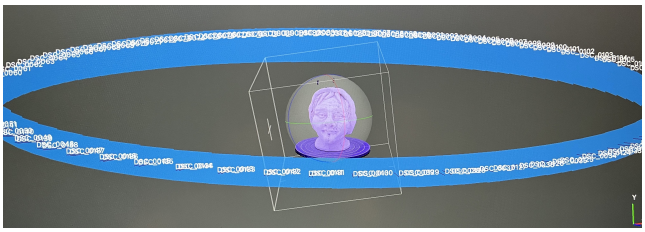

Figure 16: *Camera estimations during photogrammetry.*

As with the facial-capture workflow, Agisoft Metashape estimates a geometric mesh with textures from the input images. The mesh resolution is a lot finer and more accurate due to the large set of overlapping images from the model-scanning workflow and focus stacking. Figure 16 shows an estimate of all of the viewpoint positions from the input images during photogrammetry processing in Metashape, and the resulting digital model is shown in Figure 17.

As with the captured faces, normal, specular, and diffuse maps can be estimated for scanned models. Accurate, high-resolution texture information can be obtained such as shown in the detailed

Figure 17: *Digital model acquired through automated photogrammetry procedure from original physical sculpture by Gerry Hewett.*

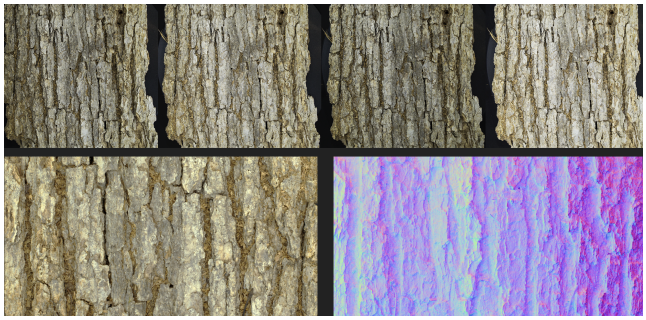

Figure 18: *Normal, specular, and diffuse information can be estimated to improve photogrammetry output for rapid asset creation.*

tree-bark images of Figure 18. Overall, VarIS facilitates high quality photogrammetry-based scanning by offering ambient, cross-polarized illumination; thousands of potential viewpoints imaged systematically; focus stacking; and potential use of active photometric techniques for additional texture detail.

3.6. Material-Acquisition Workflow

We focus on implementing the adaptive-parameterization technique [DJ18] for VarIS and extending it to support spatially varying features and transmittance by leveraging VarIS's additional capabilities. The adaptive method involves a retroreflection capture and a more complete capture for representing the material sample within the parameterization determined by processing retroreflective data. Data from retroreflection, the special case of surface reflection when the lighting and viewing directions are aligned, are used to estimate the surface roughness based on the Normal Distribution Function (NDF) term from the microfacet BRDF model [CT82] using a short sequence of measurements. Peak viewing reflectance is typically exhibited when the macro-normal is also aligned with incident light. The adaptive technique utilizes a uniform space and parameterization transforms for more efficient capture and representation; see [DJ18] for more detail.

The laser was chosen to match [DJ18] for comparison with a ring-light method that seems comparable but more favorable for

spatially varying capture. When the laser is used for capture, we attach a neutral-density (ND) filter to put the photographed pixel values in a manageable range without clipping and mount a material sample in the universal stage to be roughly aligned with the camera. The live-view GUI assists with automatically finding the retroreflection peak (where all 3 directions align). Angular resolution, the number of steps in each spherical dimension of the retroreflection directions, drives the capture. We default to 128 steps in the elevation dimension and 1 in azimuth for isotropic materials and respectively 64, 64 for anisotropic as in [DJ18].

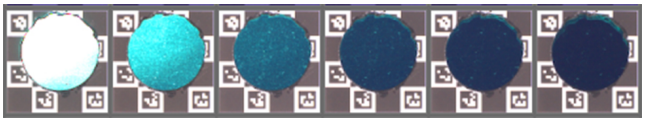

Figure 19: *A subset of rectified HDR images from a retroreflection capture of the TeckWrap "Chrome Mint" vinyl material.*

We use a single camera and choose the laser or ring light as the retroreflection accessory. The main capture sequence iterates over each set of directions, and total raw-image count is the number of directions times the number of exposures. A uniformly lit image is taken between each set to be used for image rectification per position. While the stage orients to the next measurement, the previous set of images taken are transferred from the camera storage to the desired file-system location. Images undergo HDR processing and image rectification as previously described (Figure 19). We currently sample pixels by gathering statistics from the circular sample region. We found that around 10 percent of the pixels median values represent a measurement less affected by noise and surface variation. Once an array of retroreflective measurements is obtained from the images, we perform the power-iterations technique from [DJ18] to estimate the NDF and projected-area ("sigma") terms as valued arrays across the angular dimensions. Figure 20 shows this data captured with VarIS for several different test materials.

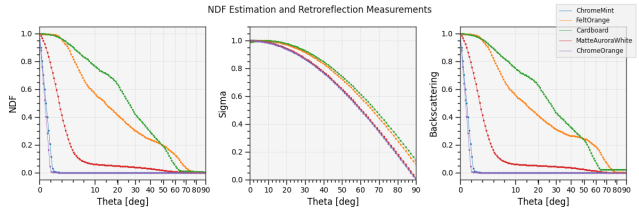

Figure 20: *Plots (based on [DJ18] of the processed Normal Distribution Function (NDF), projected area (sigma), and retroreflection data on several materials captured with VarIS.*

The main capture begins with pre-processing a tabulated visible NDF (VNDF) that drives the selection of full-capture lighting and viewing directions at a desired resolution. These directions are designed to capture material response characteristics such as a tight specular peaks on shiny surfaces or a broad, diffuse response on rough surfaces. The physical capture scheme is similar but any of the LED units on the sphere can be activated for the particular combination of directions. The viewing direction from the fixed camera is adjusted relative to the sample surface by orienting the universal stage, and we plan to investigate efficiencies that may be gained with parallel viewpoint capture in the near future. Exposure-bracketed images are taken under a chosen illuminant such as simulated D55 or D65. Proceeding the main capture, values from the processed images are sampled and arranged in 5D array to match the ".bsdf" format from [DJ18] which then can be rendered as a part of a scene with research renderers such as PBRT-v4 or Mitsuba. Figure 21 shows a sample of a few un-rectified images from a full-capture session and a final render with the measured and processed material, a TeckWrap Chrome Orange vinyl. With calibrated cameras and a tracked sample holder, we can leverage VarIS to support spatially varying measurements via clustering NDF estimations across a surface and also incorporating transmittance capture which is part of our ongoing work [BPD23]. We can also leverage the array of lights and multiple cameras to accelerate the capture process as well as investigate new methods such as incorporating MVS 3D surface methods with material-scattering measurements.

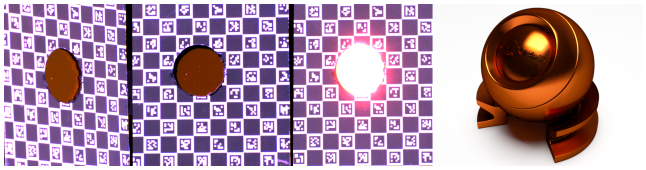

Figure 21: *A sample of un-rectified captures with the resulting render of the acquired material, Chrome Orange.*

4. Concluding Discussion

We have tested the three main applications of VarIS and continue to improve the operation and workflow with the goal of supporting a variety of research efforts. The device has also already enabled several M.F.A. thesis projects in the Digital Production Arts program at our university. We are working toward efficient capture of spatially varying and transmissive material properties and plan to continue to research and develop further automation and improvements in the various areas and other areas such as re-lighting and virtual production. We hope to investigate optimizing the use of multiple view points as well as multi-view stereo for material capture. Separately, there may be photometric methods that could improve photogrammetry workflows around model capture. We have also already begun integrating a micro-photography motorized rail system for focus stacking for near-field capture within VarIS that we hope to develop further in time. Although the system is currently primarily RGB-based, we hope to extend the spectrum and spectral sensing capabilities in the future. We've been comparing results with published data from other systems as we refine the device workflows.

Acknowledgements: This material is based upon work supported by the National Science Foundation under Grant No. 2007974. The authors would like to thank Ruben Henares, Jon Lauf, the Technical Artist team of Red Storm Entertainment, Anne Macklin, Sean Munson, Kyle Koon, Zachary Shore, Maurice Barnett, Henry Miles, Will Hendrickson, Cyprien Perrier, Eliza Sorber, Esha Kappor, and Maggie Wensink.

References

[3dm22] 3DMD. *3DMD... welcome to the 4D revolution.* May 2022. URL: https://3dmd.com/ 2.

[AG*15] ACKERMANN, JENS, GOESELE, MICHAEL, et al. "A survey of photometric stereo techniques". *Foundations and Trends® in Computer Graphics and Vision* 9.3-4 (2015), 149–254 3.

[Agi] AGISOFT. *Agisoft Metashape*. URL: https://www.agisoft.com/ 9.

[ANS] ANSI. *American National Standard ANSI E1.11 – 2008 (R2018) Entertainment Technology—USITT DMX512-A Asynchronous Serial Digital Data Transmission Standard for Controlling Lighting Equipment and Accessories*. URL: https://tsp.esta.org/tsp/documents/docs/ANSI-ESTA_E1-11_2008R2018.pdf 6.

[Api10] APIAN-BENNEWITZ, PETER. "New scanning gonio-photometer for extended BRTF measurements". *Reflection, Scattering, and Diffraction from Surfaces II*. Ed. by GU, ZU-HAN and HANSSEN, LEONARD M. Vol. 7792. International Society for Optics and Photonics. SPIE, 2010, 77920O. DOI: 10.1117/12.860889. URL: https://doi.org/10.1117/12.860889 5.

[ARN*06] AKCA, DEVRIM, REMONDINO, FABIO, NOVÁK, DAVID, et al. "Recording and modeling of cultural heritage objects with coded structured light projection systems". *2nd International Conference on Remote Sensing in Archaeology*. Institute of Geodesy and Photogrammetry, ETH Zurich. 2006, 375–382 3.

[ARV07] AMBERG, BRIAN, ROMDHANI, SAMI, and VETTER, THOMAS. "Optimal Step Nonrigid ICP Algorithms for Surface Registration". *2007 IEEE Conference on Computer Vision and Pattern Recognition*. 2007, 1–8. DOI: 10.1109/CVPR.2007.383165 2.

[Aut] AUTODESK. *Maya Help*. URL: https://help.autodesk.com/view/MAYAUL/2022/ENU/ 5, 7.

[BBB*10] BEELER, THABO, BICKEL, BERND, BEARDSLEY, PAUL, et al. "High-Quality Single-Shot Capture of Facial Geometry". *ACM Trans. Graph.* 29.4 (July 2010). ISSN: 0730-0301. DOI: 10.1145/1778765.1778777. URL: https://doi.org/10.1145/1778765.1778777 2, 9.

[Ben08] BENNETTE, ADAM. *Recommended Practice for DMX512*. 2nd ed. PLASA, 2008. ISBN: 978-0-9557035-2-2. URL: https://tsp.esta.org/tsp/documents/docs/DMX512-A_Guide_(8x10)_ESTA.PDF 6.

[BPD23] BARON, JESSICA, PATTERSON, ERIC, and DUPUY, JONATHAN. "Toward Efficient Capture of Spatially Varying Material Properties". *ACM SIGGRAPH 2023 Posters*. SIGGRAPH '23. Los Angeles, CA, USA: Association for Computing Machinery, 2023. ISBN: 9798400701528. DOI: 10.1145/3588028.3603677. URL: https://doi.org/10.1145/3588028.3603677 10.

[Bra00] BRADSKI, G. "The OpenCV Library". *Dr. Dobb's Journal of Software Tools* (2000) 7, 8.

[BV99] BLANZ, VOLKER and VETTER, THOMAS. "A morphable model for the synthesis of 3D faces". *Proceedings of the 26th annual conference on Computer graphics and interactive techniques*. 1999, 187–194 2.

[CFS*18] CHRISTENSEN, PER, FONG, JULIAN, SHADE, JONATHAN, et al. "RenderMan: An Advanced Path-Tracing Architecture for Movie Rendering". *ACM Trans. Graph.* 37.3 (Aug. 2018). ISSN: 0730-0301. DOI: 10.1145/3182162. URL: https://doi-org.libproxy.clemson.edu/10.1145/3182162 5.

[Coma] COMPANY, THE QT. *Qt Documentation*. URL: https://doc.qt.io/ 7.

[Comb] COMPUTING, RIVERBANK. *PyQt*. URL: https://www.riverbankcomputing.com/software/pyqt/ 7.

[CT82] COOK, R. L. and TORRANCE, K. E. "A Reflectance Model for Computer Graphics". *ACM Trans. Graph.* 1.1 (Jan. 1982), 7–24. ISSN: 0730-0301. DOI: 10.1145/357290.357293. URL: https://doi.org/10.1145/357290.357293 3, 9.

[Deb12a] DEBEVEC, PAUL. "The Light Stages and Their Applications to Photoreal Digital Actors". *SIGGRAPH Asia*. Singapore, Nov. 2012. URL: http://ict.usc.edu/pubs/The%20Light%20Stages%20and%20Their%20Applications%20to%20Photoreal%20Digital%20Actors.pdf 2, 4, 5.

[Deb12b] DEBEVEC, PAUL. "The light stages and their applications to photoreal digital actors". *SIGGRAPH Asia* 2.4 (2012), 1–6 2.

[DG15] DHILLON, DALJIT SINGH and GOVINDU, VENU MADHAV. "Geometric and radiometric estimation in a structured-light 3D scanner". *Machine Vision and Applications* 26 (2015), 339–352 3.

[DHT*00] DEBEVEC, PAUL, HAWKINS, TIM, TCHOU, CHRIS, et al. "Acquiring the reflectance field of a human face". *Proceedings of the 27th annual conference on Computer graphics and interactive techniques*. 2000, 145–156 2.

[DJ18] DUPUY, JONATHAN and JAKOB, WENZEL. "An Adaptive Parameterization for Efficient Material Acquisition and Rendering". *Transactions on Graphics (Proceedings of SIGGRAPH Asia)* 37.6 (Nov. 2018), 274:1–274:18. DOI: 10.1145/3272127.3275059 4, 5, 9, 10.

[DJBP23] DHILLON, DALJIT SINGH, JOSHI, PARISHA, BARON, JESSICA, and PATTERSON, ERIC K. "Robust Color Correction for Preserving Spatial Variations within Photographs". *ACM SIGGRAPH 2023 Posters*. SIGGRAPH '23. Los Angeles, CA, USA: Association for Computing Machinery, 2023. ISBN: 9798400701528. DOI: 10.1145/3588028.3603681. URL: https://doi.org/10.1145/3588028.3603681 8.

[Fac] FACEFORM. *Wrap Documentation*. URL: https://docs.faceform.com/Wrap/index.html 9.

[Gam] GAMES, EPIC. *MetaHuman Documentation*. URL: https://dev.epicgames.com/documentation/en-us/metahuman/metahuman-documentation 9.

[GFT*11] GHOSH, ABHIJEET, FYFFE, GRAHAM, TUNWATTANAPONG, BOROM, et al. "Multiview Face Capture Using Polarized Spherical Gradient Illumination". *ACM Trans. Graph.* 30.6 (Dec. 2011), 1–10. ISSN: 0730-0301. DOI: 10.1145/2070781.2024163. URL: https://doi.org/10.1145/2070781.2024163 2, 8.

[GG18] GUARNERA, DAR'YA and GUARNERA, GIUSEPPE CLAUDIO. "Virtual Material Acquisition and Representation for Computer Graphics". *Synthesis Lectures on Visual Computing* 10.1 (2018), 1–101. DOI: 10.2200/S00817ED1V01Y201711VCP030. eprint: https://doi.org/10.2200/S00817ED1V01Y201711VCP030. URL: https://doi.org/10.2200/S00817ED1V01Y201711VCP030 2, 3.

[GLL*04] GOESELE, MICHAEL, LENSCH, HENDRIK P. A., LANG, JOCHEN, et al. "DISCO: Acquisition of Translucent Objects". *ACM Trans. Graph.* 23.3 (Aug. 2004), 835–844. ISSN: 0730-0301. DOI: 10.1145/1015706.1015807. URL: https://doi.org/10.1145/1015706.1015807 5.

[Gro] GROUP, KHRONOS. *OpenGL*. URL: https://www.opengl.org/ 7.

[HBM13] HARVEY, TODD ALAN, BOSTWICK, KIMBERLY S., and MARSCHNER, STEVE. "Directional reflectance and milli-scale feather morphology of the African Emerald Cuckoo, Chrysococcyx cupreus". *J. R. Soc. Interface* (2013). DOI: http://doi.org/10.1098/rsif.2013.0391 5, 7.

[HMvdW*20] HARRIS, CHARLES R., MILLMAN, K. JARROD, van der WALT, STÉFAN J., et al. "Array programming with NumPy". *Nature* 585.7825 (Sept. 2020), 357–362. DOI: 10.1038/s41586-020-2649-2. URL: https://doi.org/10.1038/s41586-020-2649-2 7.

[HTOL20] HUANG, BINGYAO, TANG, YING, OZDEMIR, SAMED, and LING, HAIBIN. "A fast and flexible projector-camera calibration system". *IEEE Transactions on Automation Science and Engineering* 18.3 (2020), 1049–1063 3.

[HZ03] HARTLEY, RICHARD and ZISSERMAN, ANDREW. *Multiple view geometry in computer vision*. Cambridge university press, 2003 3.

[IAD13] ICHIKARI, RYOSUKE, ALEXANDER, OLEG, and DEBEVEC, PAUL. "Vuvuzela: A Facial Scan Correspondence Tool". *ACM SIGGRAPH 2013 Posters*. SIGGRAPH '13. Anaheim, California: Association for Computing Machinery, 2013. ISBN: 9781450323420. DOI: 10.1145/2503385.2503482. URL: https://doi.org/10.1145/2503385.2503482 2.

[JMLH01] JENSEN, HENRIK WANN, MARSCHNER, STEPHEN R., LEVOY, MARC, and HANRAHAN, PAT. "A Practical Model for Subsurface Light Transport". *Proceedings of the 28th Annual Conference on Computer Graphics and Interactive Techniques*. SIGGRAPH '01. New York, NY, USA: Association for Computing Machinery, 2001, 511–518. ISBN: 158113374X. DOI: 10.1145/383259.383319. URL: https://doi.org/10.1145/383259.383319 5.

[KG18] KAMPOURIS, CHRISTOS and GHOSH, ABHIJEET. "ICL Multispectral Light Stage: Building a Versatile LED Sphere with off-the-Shelf Components". *Proceedings of the Eurographics 2018 Workshop on Material Appearance Modeling*. EG MAM '18. Karlsruhe, Germany: Eurographics Association, 2018, 1–4. DOI: 10.2312/mam.20181190. URL: https://doi.org/10.2312/mam.20181190 2, 4, 5, 8.

[KRP*15] KLEHM, OLIVER, ROUSSELLE, FABRICE, PAPAS, MARIOS, et al. "Recent advances in facial appearance capture". *Computer Graphics Forum*. Vol. 34. 2. Wiley Online Library. 2015, 709–733 4.

[KZG18] KAMPOURIS, CHRISTOS, ZAFEIRIOU, STEFANOS, and GHOSH, ABHIJEET. "Diffuse-Specular Separation using Binary Spherical Gradient Illumination." *EGSR (EI&I)*. 2018, 1–10 2.

[LBK*18] LEGENDRE, CHLOE, BLADIN, KALLE, KISHORE, BIPIN, et al. "Efficient Multispectral Facial Capture with Monochrome Cameras". *ACM SIGGRAPH 2018 Posters*. SIGGRAPH '18. Vancouver, British Columbia, Canada: Association for Computing Machinery, 2018. ISBN: 9781450358170. DOI: 10.1145/3230744.3230778. URL: https://doi.org/10.1145/3230744.3230778 2, 8.

[LBSG22] LAM, TENG FOONG, BLUM, HERMANN, SIEGWART, ROLAND, and GAWEL, ABEL. "SL Sensor: An open-source, real-time and robot operating system-based structured light sensor for high accuracy construction robotic applications". *Automation in Construction* 142 (2022), 104424 3.

[Lie] LIECHTI, CHRIS. *pySerial Documentation*. URL: https://pythonhosted.org/pyserial/ 7.

[LLB*21] LI, TIANYE, LIU, SHICHEN, BOLKART, TIMO, et al. "Topologically Consistent Multi-View Face Inference Using Volumetric Sampling". *2021 IEEE/CVF International Conference on Computer Vision (ICCV)*. 2021, 3804–3814. DOI: 10.1109/ICCV48922.2021.00380 2.

[LYL*16] LEGENDRE, CHLOE, YU, XUEMING, LIU, DAI, et al. "Practical multispectral lighting reproduction". *ACM Transactions on Graphics (TOG)* 35.4 (2016), 1–11 4.

[MGW01] MALZBENDER, TOM, GELB, DAN, and WOLTERS, HANS. "Polynomial Texture Maps". *Proceedings of the 28th Annual Conference on Computer Graphics and Interactive Techniques*. SIGGRAPH '01. New York, NY, USA: Association for Computing Machinery, 2001, 519–528. ISBN: 158113374X. DOI: 10.1145/383259.383320. URL: https://doi.org/10.1145/383259.383320 4.

[MHP*07] MA, WAN-CHUN, HAWKINS, TIM, PEERS, PIETER, et al. "Rapid Acquisition of Specular and Diffuse Normal Maps from Polarized Spherical Gradient Illumination". *Proceedings of the 18th Eurographics Conference on Rendering Techniques*. EGSR'07. Grenoble, France: Eurographics Association, 2007, 183–194. ISBN: 9783905673524 2, 6, 8.

[MJC*03] MARSCHNER, STEPHEN R., JENSEN, HENRIK WANN, CAMMARANO, MIKE, et al. "Light Scattering from Human Hair Fibers". *ACM SIGGRAPH 2003 Papers*. SIGGRAPH '03. San Diego, California: ACM, 2003, 780–791. ISBN: 1-58113-709-5. DOI: 10.1145/1201775.882345. URL: http://doi.acm.org/10.1145/1201775.882345 5.

[MMP*22] MANSENCAL, THOMAS, MAUDERER, MICHAEL, PARSONS, MICHAEL, et al. *Colour 0.4.3*. Version 0.4.3. Nov. 2022. DOI: 10.5281/zenodo.8284953. URL: https://doi.org/10.5281/zenodo.8284953 7, 8.

[MPBM03] MATUSIK, WOJCIECH, PFISTER, HANSPETER, BRAND, MATTHEW, and MCMILLAN, LEONARD. "Efficient Isotropic BRDF Measurement". *Proceedings of the 14th Eurographics Workshop on Rendering*. EGRW '03. Leuven, Belgium: Eurographics Association, 2003, 241–247. ISBN: 3905673037 4, 5.

[MT12] MORENO, DANIEL and TAUBIN, GABRIEL. "Simple, accurate, and robust projector-camera calibration". *2012 Second International Conference on 3D Imaging, Modeling, Processing, Visualization & Transmission*. IEEE. 2012, 464–471 3.

[MWL*99] MARSCHNER, STEPHEN R., WESTIN, STEPHEN H., LAFORTUNE, ERIC P. F., et al. "Image-Based BRDF Measurement Including Human Skin". *Rendering Techniques' 99*. Ed. by LISCHINSKI, DANI and LARSON, GREG WARD. Vienna: Springer Vienna, 1999, 131–144. ISBN: 978-3-7091-6809-7 5.

[PBS18] PATTERSON, ERIC, BARON, JESSICA, and SIMPSON, DEVIN. "Landmark-Based Re-topology of Stereo-Pair Acquired Face Meshes". *Computer Vision and Graphics: International Conference, ICCVG 2018, Warsaw, Poland, September 17-19, 2018, Proceedings*. Springer. 2018, 425–437 2.

[pdtea20] Pandas development TEAM, THE. *pandas-dev/pandas: Pandas*. Version latest. Feb. 2020. DOI: 10.5281/zenodo.3509134. URL: https://doi.org/10.5281/zenodo.3509134 7.

[PG07] PENG, TAO and GUPTA, SATYANDRA K. "Model and algorithms for point cloud construction using digital projection patterns". (2007) 3.

[Pli] PLICA, MATHIAS. *Craftcloud by All3DP*. URL: https://craftcloud3d.com/ 6.

[PSQ06] PARIS, SYLVAIN, SILLION, FRANÇOIS X, and QUAN, LONG. "A surface reconstruction method using global graph cut optimization". *International Journal of Computer Vision* 66 (2006), 141–161 3.

[RCM*01] ROCCHINI, CMPPC, CIGNONI, PAULO, MONTANI, CLAUDIO, et al. "A low cost 3D scanner based on structured light". *computer graphics forum*. Vol. 20. 3. Wiley Online Library. 2001, 299–308 3.

[RE06] REMONDINO, FABIO and EL-HAKIM, SABRY. "Image-based 3D modelling: a review". *The photogrammetric record* 21.115 (2006), 269–291 2.

[Rus98] RUSINKIEWICZ, SZYMON. "A New Change of Variables for Efficient BRDF Representation". *Rendering Techniques (Proc. Eurographics Workshop on Rendering)*. June 1998 4, 5.

[SD99] SEITZ, STEVEN M and DYER, CHARLES R. "Photorealistic scene reconstruction by voxel coloring". *International Journal of Computer Vision* 35 (1999), 151–173 3.

[Son] SONOSTAR. *Sonostar Universal Structures*. URL: https://www.sonostarhub.com 5.

[SWM*16] SHI, BOXIN, WU, ZHE, MO, ZHIPENG, et al. "A benchmark dataset and evaluation for non-lambertian and uncalibrated photometric stereo". *Proceedings of the IEEE Conference on Computer Vision and Pattern Recognition*. 2016, 3707–3716 3.

[TS67] TORRANCE, K. E. and SPARROW, E. M. "Theory for Off-Specular Reflection From Roughened Surfaces*". *J. Opt. Soc. Am.* 57.9 (Sept. 1967), 1105–1114. DOI: 10.1364/JOSA.57.001105. URL: http://www.osapublishing.org/abstract.cfm?URI=josa-57-9-1105 3.

[VGO*20] VIRTANEN, PAULI, GOMMERS, RALF, OLIPHANT, TRAVIS E., et al. "SciPy 1.0: Fundamental Algorithms for Scientific Computing in Python". *Nature Methods* 17 (2020), 261–272. DOI: 10.1038/s41592-019-0686-2 7.

[WLL*08] WEYRICH, TIM, LAWRENCE, JASON, LENSCH, HENDRIK, et al. "Principles of appearance acquisition and representation". *Foundations and Trends in Computer Graphics and Vision* 4.2 (2008), 75–191. DOI: http:/dx.doi.org/10.1561/0600000022 3.

[WMP*06] WEYRICH, TIM, MATUSIK, WOJCIECH, PFISTER, HANSPETER, et al. "Analysis of Human Faces Using a Measurement-Based Skin Reflectance Model". *ACM Trans. Graph.* 25.3 (July 2006), 1013–1024. ISSN: 0730-0301. DOI: 10.1145/1141911.1141987. URL: https://doi.org/10.1145/1141911.1141987 2, 5.

[WNRM15] WAUGH, TIM, NIEDERMANN, HANS ULRICH, RENSING, MICHAEL J., and MEISSNER, MARCUS. *The gPhoto2 Manual*. 2015. URL: http://gphoto.org/doc/manual/ 6, 7.

[Woo80] WOODHAM, ROBERT J. "Photometric method for determining surface orientation from multiple images". *Optical engineering* 19.1 (1980), 139–144 3.

[Woo84] WOODHAM, ROBERT J. *Photometric method for determining shape from shading*. University of British Columbia, 1984 3.

[Zha12] ZHANG, ZHENGYOU. "Microsoft kinect sensor and its effect". *IEEE multimedia* 19.2 (2012), 4–10 3.

[ZXX*14] ZHANG, CHI, XU, JING, XI, NING, et al. "A Robust Surface Coding Method for Optically Challenging Objects Using Structured Light". *IEEE Transactions on Automation Science and Engineering* 11.3 (2014), 775–788. DOI: 10.1109/TASE.2013.2293576 3.

[ZZC*23] ZHANG, LONGWEN, ZHAO, ZIJUN, CONG, XINZHOU, et al. "HACK: Learning a Parametric Head and Neck Model for High-Fidelity Animation". *ACM Trans. Graph.* 42.4 (July 2023). ISSN: 0730-0301. DOI: 10.1145/3592093. URL: https://doi.org/10.1145/3592093 2.

[ZZG07] ZHANG, XIAOZHENG, ZHAO, SANQIANG, and GAO, YONGSHENG. "Lighting Analysis and Texture Modification of 3D Human Face Scans". *9th Biennial Conference of the Australian Pattern Recognition Society on Digital Image Computing Techniques and Applications (DICTA 2007)*. 2007, 402–407. DOI: 10.1109/DICTA.2007.4426825 2.

[ZZZ*22] ZHANG, LONGWEN, ZENG, CHUXIAO, ZHANG, QIXUAN, et al. "Video-Driven Neural Physically-Based Facial Asset for Production". *ACM Trans. Graph.* 41.6 (Nov. 2022). ISSN: 0730-0301. DOI: 10.1145/3550454.3555445. URL: https://doi.org/10.1145/3550454.3555445 2.